Multiple-Quantum Line Narrowing for Measurement of $H^{\alpha}-H^{\beta}$ J Couplings in Isotopically Enriched Proteins

Stephan Grzesiek,*,† Hitoshi Kuboniwa,† Andrew P. Hinck,‡ and Ad Bax*,†

Contribution from the Laboratory of Chemical Physics, National Institutes of Diabetes and Digestive and Kidney Diseases, and Molecular Structural Biology Unit, Office of the Director of the National Institute of Dental Research, National Institutes of Health, Bethesda, Maryland 20892-0520

Received January 11, 1995[⊗]

Abstract: Uniform ^{13}C enrichment of proteins is commonly used for NMR studies of proteins that are not amenable to conventional homonuclear 2D NMR spectroscopy. In such studies, the one-bond $^{1}H-^{13}C$ dipolar interaction is usually the dominant source of ^{1}H line broadening. $^{1}H-^{13}C$ zero- and double-quantum coherences are, to first order, not affected by this dipolar relaxation mechanism. The relatively long relaxation time of such $^{1}H^{\alpha}-^{13}C^{\alpha}$ multiple-quantum coherences is exploited for measurement of $H^{\alpha}-H^{\beta}$ J couplings in a sample of uniformly ^{13}C-enriched calcium-free calmodulin (16.7 kD) and a sample of TGF-β1 (25 kDa). $J(H^{\alpha}-H^{\beta})$ provides information on the stereospecific resonance assignment for residues with nonequivalent H^{β} methylene protons and on the χ_1 torsion angles.

Uniform ^{13}C enrichment of proteins makes it possible to record highly sensitive 3D and 4D analogs of conventional 2D COSY, TOCSY, and NOESY NMR spectra.[1,2] Spectral dispersion in the added ^{13}C dimension(s) greatly alleviates the resonance overlap problem of conventional 2D NMR and makes it possible to study the structure of proteins in the 10−30 kDa range. However, enrichment with ^{13}C has a deleterious effect on the ^{1}H line width, resulting from the large one-bond $^{1}H-^{13}C$ dipolar coupling which, in diamagnetic proteins, represents the dominant source of transverse ^{1}H relaxation. In the slow tumbling limit, relaxation of $^{1}H-^{13}C$ zero- and double-quantum coherence is, to first order, not influenced by the dipolar coupling between the two nuclei.[3] In macromolecules the relaxation time of one-bond $^{1}H-^{13}C$ zero- and double-quantum coherence therefore is expected to be longer than for the single-quantum coherence of the individual ^{1}H and ^{13}C spins. An analogous increase in the relaxation time of $^{1}H-^{15}N$ multiple-quantum coherence over the amide proton T_2 was exploited to obtain a modest increase in $H^{N}-H^{\alpha}$ COSY cross peak intensities of ^{15}N-enriched proteins,[4] and for minimizing signal loss in $^{3}J(H^{N}-H^{\alpha})$-modulated $^{1}H-^{15}N$ shift correlation experiments, aimed at measurement of $^{3}J(H^{N}-H^{\alpha})$.[5,6] For $^{1}H-\{^{13}C\}$, the heteronuclear dipolar broadening is about four times larger and therefore the difference between multiple-quantum and single-quantum relaxation is also much larger.[7,8] Here we demonstrate that use of $^{1}H-^{13}C$ multiple-quantum coherence indeed results in a large enhancement of resonance intensities in a quantitative $H^{\alpha}-H^{\beta}$ J correlation spectrum. Such a spectrum yields quantitative values for three-bond $H^{\alpha}-H^{\beta}$ J couplings, $J_{\alpha\beta}$, which are important for stereospecific assignment of nonequivalent C^{β} methylene protons and provide information on the side chain χ_1 torsion angles.

Description of the Pulse Scheme

The pulse scheme for the 3D $^{13}C^{\alpha}$-separated $H^{\alpha}-H^{\beta}$ in-phase COSY (HACAHB-COSY) pulse sequence is shown in Figure 1. Analogous to the HNHA experiment,[9] proposed for measurement of $^{3}J(H^{N}-H^{\alpha})$, the HACAHB-COSY scheme produces in-phase cross peaks and diagonal peaks, and the ratio of their integrated intensities provides a direct measure for $J_{\alpha\beta}$.[10,11] The operator formalism description of this experiment is analogous to that of the HNHA experiment, and a detailed description is therefore not repeated.

The HACAHB-COSY scheme is of the so-called "out-and-back" type,[12] where magnetization originates on H^{α} and is also detected as H^{α} magnetization during data acquisition. Briefly, the experiment functions as follows: The first $90_{\phi_1}(^{1}H)-\Delta-90_{x}(^{13}C)$ pulse pair converts H^{α} magnetization into a heteronuclear $H^{\alpha}{}_{x}C^{\alpha}{}_{y}$ spin operator product wich represents the sum of $H^{\alpha}-C^{\alpha}$ zero- and double-quantum coherence. Temporarily ignoring the effect of $^{13}C^{\alpha}$ chemical shift evolution, this coherence dephases between time points a and c due to homonuclear $H^{\alpha}-H^{\beta}$ J coupling, resulting in an operator product of the form $H^{\alpha}{}_{y}C^{\alpha}{}_{y}H^{\beta}{}_{z}$, in addition to the non-dephased component $H^{\alpha}{}_{x}C^{\alpha}{}_{y}$. The relative amplitude of these two coherences is $\tan(2\pi J_{\alpha\beta}\delta)$. The subsequent $90_{\phi_1}-t_2-90_{\phi_4}$ sequence, applied

† Laboratory of Chemical Physics.
‡ Molecular Structural Biology Unit.
[⊗] Abstract published in *Advance ACS Abstracts,* May 1, 1995.

(1) Clore, G. M.; Gronenborn, A. M. *Prog. NMR. Spectrosc.* **1991**, *23*, 43−92.
(2) Edison, A. S.; Abildgaard, F.; Westler, W. M.; Mooberry, E. S.; Markley, J. L. *Meth. Enzymol.* **1993**, *239*, 3−79.
(3) Griffey, R. H.; Redfield, A. G. *Q. Rev. Biophys.* **1987**, *19*, 51−82.
(4) Bax, A.; Kay, L. E.; Sparks, S. W.; Torchia, D. A. *J. Am. Chem. Soc.* **1989**, *111*, 408−409.
(5) Billeter, M.; Neri, D.; Otting, G.; Qian, Y. Q.; Wüthrich, K. *J. Biomol. NMR* **1992**, *2*, 257−274.
(6) Kuboniwa, H.; Grzesiek, S.; Delaglio, F.; Bax, A. *J. Biomol. NMR* **1994**, *4*, 871−878.
(7) Bax, A.; Ikura, M.; Kay, L. E.; Torchia, D. A.; Tschudin, R. *J. Magn. Reson.* **1990**, *86*, 304−318.
(8) Seip, S.; Balbach, J.; Kessler, H. *J. Magn. Reson.* **1992**, *100*, 406−410.
(9) Vuister, G. W.; Bax, A. *J. Am. Chem. Soc.* **1993**, *115*, 7772−7777.
(10) Bax, A.; Max, D.; Zax, D. *J. Am. Chem. Soc.* **1992**, *114*, 6924−6925.
(11) Bax, A.; Vuister, G. W.; Grzesiek, S.; Delaglio, F.; Wang, A. C.; Tschudin, R.; Zhu, G. *Meth. Enzymol.* **1993**, *239*, 79−105.
(12) Ikura, M.; Kay, L. E.; Bax, A. *Biochemistry* **1990**, *29*, 4659−4667.

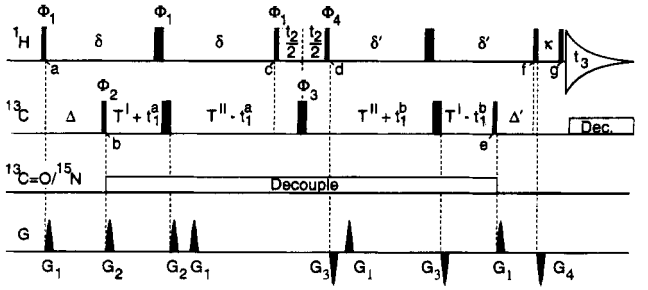

Figure 1. Pulse scheme for the 3D HACAHB-COSY experiment. Narrow and wide pulses denote 90° and 180° flip angles, respectively. Unless indicated otherwise, all pulses are applied along the x-axis. The phase cycle is as follows: $\phi_1 = 2(x),2(-x)$; $\phi_2 = x$; $\phi_3 = x,y,-x,-y$; $\phi_4 = 4(x), 4(-x)$; receiver $= x,2(-x),x$. Quadrature detection in t_1 and t_2 is obtained by incrementing ϕ_2 and ϕ_1, using States-TPPI. ^{13}CO decoupling is preferably carried out with a selective composite pulse decoupling scheme,[20,25] but due to hardware problems a 2 kHz CW field was used instead. Note that ^{13}CO decoupling during t_1 induces a significant Bloch–Siegert shift (~0.7 ppm) in F_1. Delay durations: $\kappa = 1.5$ ms; $T^{I} = 5.25$ ms; $T^{II} = 8.75$ ms; $\delta = T^{II} + 2\tau_{90}^{C}$; $\delta' = T^{II} - 2\tau_{90}^{H}$; $\Delta = \delta + 2\tau_{90}^{H} - T^{I} - \tau_{90}^{C}$; $\Delta' = \delta' - T^{I} - 3\tau_{90}^{C}$, where τ_{90}^{C} and τ_{90}^{H}, are the 90° ^{13}C and ^{1}H pulse durations. Pulsed field gradients (PFG) are all sine-bell shaped with a strength of 25 G/cm at their midpoint and durations of $G_{1,2,3,4} = 0.3$, 0.4, 0.6, and 0.25 ms. The ^{13}C carrier is positioned at 46 ppm, the ^{13}CO carrier at 177 ppm, and the ^{15}N carrier at 116.5 ppm.

between time points c and d, modulates the amplitude of these terms:

$$H^{\alpha}{}_{x}C^{\alpha}{}_{y} \rightarrow \cos(\omega_{\alpha}T_2)H^{\alpha}{}_{x}C^{\alpha}{}_{y} \quad (1a)$$

$$H^{\alpha}{}_{y}C^{\alpha}{}_{y}H^{\beta}{}_{z} \rightarrow \cos(\omega_{\beta}t_2)H^{\alpha}{}_{y}C^{\alpha}{}_{y}H^{\beta}{}_{z} \quad (1b)$$

where ω_{α} and ω_{β} are the angular offset frequencies of the H^{α} and H^{β} spins. As discussed below, the effect of homonuclear J-dephasing during the short t_2 evolution periods (*ca.* 12 ms, in practice) is very small and has therefore been ignored in eq 1. During the subsequent delay, $2\delta'$, a $\cos(2\pi J_{\alpha\beta}\delta')$ fraction of the product in eq 1a is converted back to in-phase $H^{\alpha}{}_{y}$ magnetization at time point f and, similarly, a $-\sin(2\pi J_{\alpha\beta}\delta')$ fraction of eq 1b is converted back to in-phase $H^{\alpha}{}_{y}$. Thus, at time f there are two contributions to the in-phase $H^{\alpha}{}_{y}$ magnetization: a $\cos(2\pi J_{\alpha\beta}\delta)\cos(2\pi J_{\alpha\beta}\delta')$ fraction is modulated in amplitude by $\cos(\omega_{H\alpha}t_2)$ and gives rise to a diagonal resonance, and a $-\sin(2\pi J_{\alpha\beta}\delta)\sin(2\pi J_{\alpha\beta}\delta')$ fraction is modulated by $\cos(\omega_{H\beta}t_2)$, yielding the $H^{\alpha}-H^{\beta}$ cross peak. In order to eliminate other terms, which have been ignored in the above discussion, this magnetization is subjected to a z filter[13] prior to detection (between times f and g). The relative amplitude of the cross peak (I_C) versus diagonal peak (I_D) is

$$I_C/I_D = -\tan(2\pi J_{\alpha\beta}\delta)\tan(2\pi J_{\alpha\beta}\delta') \approx -\tan^2[\pi J_{\alpha\beta}(\delta + \delta')] \quad (2)$$

Between time points b and c and between d and e, $^{13}C^{\alpha}$ spin operators are part of $^{1}H^{\alpha}-^{13}C^{\alpha}$ multiple-quantum coherence and $^{1}J_{H\alpha C\alpha}$ therefore has no effect on the evolution of the spin system. Also, as was the case for the ^{15}N spin in the HNHA experiment,[9] it is easily seen that long-range J coupling between $^{13}C^{\alpha}$ and H^{β} does not give rise to observable magnetization and merely results in a small attenuation of both diagonal and cross peaks. Similarly, in the case where there are two nonequivalent methylene protons, $H^{\beta 2}$ and $H^{\beta 3}$, J coupling between H^{α} and $H^{\beta 3}$ attenuates both the diagonal resonance and the $H^{\alpha}/H^{\beta 2}$ cross peak by the same factor, $\cos(2\pi J_{\alpha\beta 3}\delta)\cos(2\pi J_{\alpha\beta 3}\delta')$, leaving eq 2 unchanged. Analogously, if the amide proton has not been exchanged with D_2O, both the diagonal and H^{α}/H^{β} cross peaks are attenuated by $\cos(2\pi J_{H\alpha HN}\delta)\cos(2\pi J_{H\alpha HN}\delta')$, again leaving the diagonal to cross peak intensity ratio unchanged. In this latter case, there will also be a $H^{N}-H^{\alpha}$ cross peak with an I_C/I_D ratio given again by eq 2, but substituting $J_{H\alpha HN}$ for $J_{\alpha\beta}$. Note, however, that the HACAHB-COSY experiment is performed preferably in D_2O solution because suppression of the H_2O solvent resonance is non-trivial.

Evolution of the $^{13}C^{\alpha}$ chemical shift between time points b and e gives rise to a modulation of the observed signal by $\cos[\omega_{C\alpha}(2t_1{}^{a} + 2t_1{}^{b})]$ which is used to disperse the $H^{\alpha}-H^{\beta}$ correlations into a third frequency dimension. The optimal choice of T^{I} and T^{II} is dictated by the requirement that $2(T^{I} + T^{II}) = n/J_{CC}$ with (n = 1, 2, ...), where J_{CC} is the one-bond $^{13}C^{\alpha}-^{13}C^{\beta}$ J coupling (~35 Hz). For programming convenience it is also desirable that $\delta' < T^{II} < \delta$ and $\delta - \Delta < T^{I} < \delta' - \Delta'$. The t_1 evolution period is of the constant-time type,[14] and J_{CC} evolution causes no t_1 modulation. However, this coupling is active during t_2, resulting in a J_{CC} doublet splitting in the indirectly detected ^{1}H dimension. As the maximum t_2 duration is typically chosen shorter than $1/(2J_{CC})$, this splitting remains unresolved and merely limits the resolution obtainable in F_2. H^{α}/H^{β} cross peaks to nonequivalent H^{β} resonances that differ by less than *ca.* 0.1 ppm are therefore generally not resolved and the corresponding J values cannot be measured individually.

Pulsed Field Gradients. The intrinsic sensitivity of the HACAHB-COSY experiment is quite good, and the resolution in the $^{13}C^{\alpha}$ dimension is also very high, provided that the entire duration of the constant-time t_1 evolution period (~28 ms) is utilized. This latter condition requires the use of a large number of increments in the t_1 dimension and, to keep the measurement time within reasonable limits, it is necessary to restrict the phase cycling to at most eight steps. Therefore, pulsed field gradients are used in the standard manner[15,16] to minimize artifacts associated with pulse imperfections. Specifically, the first 180° ^{1}H pulse is sandwiched between two pairs of gradient pulses, G_1 and G_2, so that at time c only magnetization that has been refocused by this 180° pulse is present. Similarly, the last 180° ^{1}H pulse is preceded and followed by gradients G_3 and G_1, so that at time f all ^{1}H terms of interest are refocused. As G_3 and G_1 are of opposite phase, their sum is smaller than the largest of these two gradients (G_3) but still sufficient to dephase any ^{1}H terms that have not experienced the last 180° ^{1}H pulse. On the ^{13}C channel, the first 180° pulse is surrounded by gradients G_2, the $180°_{\phi_3}$ pulse by gradients G_1, and the last 180° pulse by gradients G_3. Finally, gradient G_4, applied during the z filter delay, eliminates any non-longitudinal terms, except for possible small amounts of homonuclear zero-quantum coherence.

Effects of Relaxation and Passive J Coupling. Equation 2 applies to the ratio of the integrated peak intensities. The line shapes in the $F_1(^{13}C^{\alpha})$ and $F_3(^{1}H^{\alpha})$ dimensions are identical for cross peaks and diagonal peaks, however. As shown below, the line shape in the F_2 dimension is primarily determined by the short duration of the t_2 acquisition time needed to avoid introduction of a $^{1}J_{C\alpha C\beta}$ splitting in this dimension. The signal in the t_2 dimension decays as a result of transverse relaxation and dephasing caused by $^{1}J_{C\alpha C\beta}$ and $^{1}H-^{1}H$ J couplings. Although this decay does not change the integrated intensity, it attenuates the height of the H^{β} cross peak relative to the H^{α}

(13) Sørensen, O. W.; Rance, M.; Ernst, R. R. *J. Magn. Reson.* **1984**, *56*, 527–534.

(14) Santoro, J.; King, G. C. *J. Magn. Reson.* **1992**, *97*, 202–207.

(15) Bax, A.; Pochapsky, S. S. *J. Magn. Reson.* **1992**, *99*, 638–643.

(16) Wider, G.; Wüthrich, K. *J. Magn. Reson. Ser. B* **1993**, *102*, 239–241.

diagonal peak by a factor C, given by

$$C = \int_{t_2=0}^{AT_2} \Pi_k \cos(\pi J_{\beta k} t_2) \cos(\pi J_{CC} t_2)\, F(t_2)$$
$$\exp(-t_2/T_{2\beta})\, dt_2 / \int_{t_2=0}^{AT_2} \Pi_l \cos(\pi J_{\alpha l} t_2) \cos(\pi J_{CC} t_2)\, F(t_2)$$
$$\exp(-t_2/T_{2\alpha,MQ})\, dt_2 \quad (3)$$

where the first product extends over all protons, k, that are coupled to H^β, including H^α and H^γ protons and a possible geminal $H^{\beta'}$ spin. The second product extends over all protons, l, coupled to H^α. AT_2 is the acquisition time in the t_2 dimension, J_{CC} is the one-bond $^{13}C^\alpha-^{13}C^\beta$ J coupling, $T_{2\beta}$ and $T_{2\alpha,MQ}$ are the transverse relaxation times of H^β and $H^\alpha-C^\alpha$ two-spin coherence, and $F(t_2)$ is the digital filter applied to the t_2 time domain. Using $AT_2 = 12$ ms, a cosine bell $F(t_2)$ filter, $T_{2\beta} = 30$ ms, and $T_{2\alpha,MQ} = 100$ ms, one finds from expression 3 that even in the unfavorable case of a valine residue, with six H^γ protons ($J_{\beta\gamma} = 7$ Hz) and a $J_{\alpha\beta}$ value of 10 Hz, the value of C (0.89) is only little affected by the passive spin couplings and transverse relaxation. For a shorter $T_{2\beta}$ value of 15 ms and $T_{2\alpha,MQ} = 50$ ms, C reduces to 0.83. In practice C is dominated by the effect of $T_{2\beta}$; in the absence of T_2 relaxation one finds $C = 0.97$ for this valine spin system. The above example illustrates that the cross peak to diagonal peak height ratio in practice will be attenuated by 3−17% relative to the ratio of the integrated intensities, resulting in underestimates of $J_{\alpha\beta}$ by 2−8%. As, in our experience, the peak heights can be measured more reliably than their integrated intensities, particularly in the case of partial overlap, we prefer deriving $J_{\alpha\beta}$ from the ratio of the peak heights, rather than from the integrated intensities. As argued above, the error introduced by the difference in F_2 line width of the diagonal and cross peaks is small and can be accounted for easily.

A more serious source of error in quantitating $J_{\alpha\beta}$ couplings from the HACAHB-COSY spectrum stems from the faster relaxation of antiphase magnetization relative to in-phase coherence during the de- and rephasing periods, 2δ and $2\delta'$: The diagonal peaks result from terms, $H^\alpha{}_x C^\alpha{}_y$, that are in-phase relative to H^β during the 2δ and $2\delta'$ periods (eq 1a). $H^\alpha-H^\beta$ cross peaks result from terms that become antiphase with respect to H^β ($H^\alpha{}_y C^\alpha{}_y H^\beta{}_z$) during the period 2δ and that return to in-phase during $2\delta'$ (eq 1b). Due to relatively rapid $^1H-^1H$ spin flips in proteins, the faster relaxation of $H^\alpha{}_y C^\alpha{}_y H^\beta{}_z$ compared to $H^\alpha{}_x C^\alpha{}_y$ can result in a significant attenuation of the cross peak relative to the diagonal peak. This effect has previously been described in detail for the HNHA experiment,[9] and for quantitating the J coupling between Leu $^{13}C^\delta$ and $^1H^\beta$.[17] It increases approximately linearly with the rotational correlation time of the protein and results in an underestimate of the J coupling. This is a general phenomenon that applies to nearly all types of J coupling measurements in macromolecules.[18] For the case of two nonequivalent methylene protons, $H^{\beta2}$ and $H^{\beta3}$, rapid $H^{\beta2}-H^{\beta3}$ spin flips can actually convert $H^\alpha{}_y C^\alpha{}_y H^{\beta2}{}_z$ antiphase terms into $H^\alpha{}_y C^\alpha{}_y H^{\beta3}{}_z$, thereby decreasing the intensity of the largest cross peak but increasing the intensity of the weaker of the two $H^\alpha-H^\beta$ cross peaks.[17] Numerical calculations based on equations in refs 9 and 17 indicate that for a protein with a rotational correlation time of 7 ns and a generalized order parameter, S^2, of 0.8, a *trans* $J_{\alpha\beta2}$ coupling to a $H^{\beta2}$ methylene proton is underestimated by ~15−20%. The magnitude of the measured value for the smaller *gauche* coupling, $J_{\alpha\beta3}$, is less affected in such cases as the increase of $H^\alpha{}_y C^\alpha{}_y H^{\beta3}{}_z$ caused by $H^{\beta2}-H^{\beta3}$ spin flips is partially offset by a decrease caused by spin flips between $H^{\beta3}$ and protons other than H^α and $H^{\beta2}$.

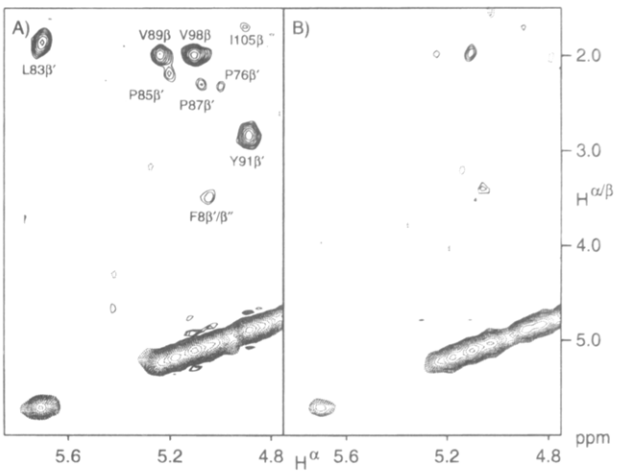

Figure 2. Comparison of a small region of the 600 MHz 2D in-phase HACAHB-COSY spectrum of TGF-β1, recorded (A) with the scheme of Figure 1, without incrementing t_1, and (B) with a single-quantum analog of this experiment (see Experimental Section). Diagonal and cross peaks have opposite signs.[9−11]

Results and Discussion

The improvement in the relaxation behavior of $^1H-^{13}C$ multiple-quantum coherence over single-quantum coherence is demonstrated for a sample of the homodimeric protein TGF-β1 (25 kDa). The protein has been derived from mammalian cells and only about half of its residues are enriched in ^{13}C. Figure 2A shows a small region of the in-phase 2D $^1H-^1H$ COSY spectrum, recorded with the scheme of Figure 1. Strips taken from the corresponding 3D spectrum are given as supplementary material. As the spectrum shown in Figure 2 is not dispersed in the ^{13}C dimension, most of the diagonal H^α resonances overlap but numerous intense cross peaks to previously assigned[19] H^β resonances are well resolved. In contrast, if the experiment is carried out without generating heteronuclear multiple-quantum coherence (Figure 2B), diagonal resonances are approximately 4-fold weaker and, except for V98 and V89, cross peaks fall below the noise threshold. The slower relaxation rate applies to the period $2(T^{\mathrm{I}} + T^{\mathrm{II}})$, which equals 28 ms, indicating a heteronuclear $^1H^\alpha-^{13}C^\alpha$ dipolar contribution to the H^α transverse relaxation rate of $\ln(4)/0.028 \approx 50\ s^{-1}$, corresponding to a rotational correlation time of ~12 ns. This correlation time falls in the range expected for a 25 kDa protein and the decrease in relaxation therefore agrees with theoretical predictions.

The use of the 3D HACAHB-COSY scheme for measurement of $J_{\alpha\beta}$ is illustrated for a sample of uniformly ^{13}C-enriched Ca^{2+}-free calmodulin (148 residues) at 23 °C. This protein presents a more challenging test for the practical use of the method than TGF-β1, because it has been enriched uniformly in ^{13}C, and in the absence of Ca^{2+} the $^1H^\alpha-^{13}C^\alpha$ correlation spectrum of this highly α-helical protein is very poorly dispersed. Figure 3 shows F_2 strips taken from the 3D spectrum at the $^{13}C^\alpha$ (F_1) and $^1H^\alpha$ (F_3) frequencies of residues Q41−I52. For Q41, for example, the $H^\alpha-H^{\beta2}$ cross peak intensity corresponds to $J_{\alpha\beta2} = 9.3$ Hz. The absence of an $H^\alpha-H^{\beta3}$ cross peak, even at lower contour levels, indicates that $J_{\alpha\beta3} < 3.5$ Hz, diagnostic of a *gauche* coupling.

(17) Vuister, G. W.; Yamazaki, T.; Torchia, D. A.; Bax, A. *J. Biomol. NMR* **1993**, *3*, 297−306.
(18) Harbison, G. *J. Am. Chem. Soc.* **1993**, *115*, 3026−3027.
(19) Archer, S. J.; Bax, A.; Roberts, A. B.; Sporn, M. B.; Ogawa, Y.; Piez, K. A.; Weatherbee, J. A.; Tsang, M. L.-S.; Lucas, R.; Zheng, B.-L.; Wenker, J.; Torchia, D. A. *Biochemistry* **1993**, *32*, 1152−1163.

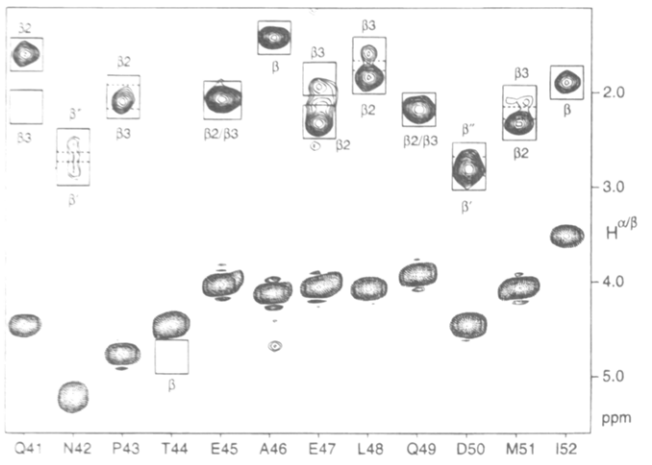

Figure 3. F_2 strips from the 600 MHz 3D HACAHB-COSY spectrum of 1.7 mM Ca^{2+}-free calmodulin in D_2O. The center of each square box indicates the position of a H^{β} resonance. Overlapping boxes are partially dashed. Thus, even though the H^{β} protons of Pro^{43} are not resolved, it is clear that the J coupling is larger to $H^{\beta 3}$ than to $H^{\beta 2}$. The diagonal and cross peaks of Glu^{47} partially overlap with those of Glu^{87} and Glu^{140}. A total of 114 $J_{\alpha\beta}$ couplings could be measured quantitatively, and for 37 cases the absence of a cross peak indicated $J_{\alpha\beta} <$ ~4 Hz.

$J_{\alpha\beta}$ values measured from the 3D spectrum for 10 of the alanines in the ordered region of calmodulin all fall in the 5.6–6.2 Hz range, substantially below the 7 Hz value expected for this coupling. In contrast, the intensity ratio for the highly mobile N-terminal alanine indicates a value of 6.9 Hz. The same experiment applied to human ubiquitin, which has a relatively fast rotational correlation time of *ca.* 4.5 ns, yielded $J_{\alpha\beta}$ values of 6.5 Hz for its two alanines. As discussed above, this reduction in the measured J coupling relative to its true value is caused by the faster relaxation of antiphase terms, compared to in-phase magnetization, which results in a decrease of the cross peak to diagonal peak intensity ratio. Except for highly mobile residues, which are easily recognized because of their very intense diagonal intensity, the underestimate of the $J_{\alpha\beta}$ coupling caused by this relaxation effect is relatively uniform throughout the protein. Nearly all methods for measurement of small J couplings in proteins are affected by the faster relaxation of antiphase versus in-phase magnetization.[18] Comparison of the $J_{\alpha\beta}$ values measured in human ubiquitin using the HACAHB-COSY scheme with the values obtained from a $^{13}C^{\alpha}$ separated E. COSY scheme[20] indicates that the HACAHB-COSY data are less affected by this relaxation effect than the corresponding E. COSY spectra (A. C. Wang, unpublished results).

In combination with heteronuclear $^{15}N-^{1}H^{\beta}$ and $^{13}C'-^{1}H^{\beta}$ three-bond J couplings and/or NOE cross peak intensities, $J_{\alpha\beta}$ values can be used for making stereospecific assignments of the H^{β} methylene protons and for determining the rotameric states around the $C^{\alpha}-C^{\beta}$ bonds in proteins. Although other methods for measuring this coupling have been described in recent years,[20-22] for larger proteins the present method in our experience compares favorably in sensitivity and in spectral simplicity. The data presented in Figure 2 convincingly demonstrate the gain in sensitivity that can be obtained by using the slower relaxation rate of $^{1}H-^{13}C$ multiple-quantum coherence compared to that of the ^{1}H single-quantum coherence. The same idea can be incorporated in numerous other multi-dimensional heteronuclear NMR experiments and may further increase the size limit of proteins that can be studied in detail by multi-dimensional heteronuclear NMR.

Experimental Section

The sample of TGF-β1 was obtained from overexpression in Chinese hamster ovary cells, grown on a medium containing uniformly $^{15}N/^{13}C$-enriched Leu, Ile, Val, Pro, Tyr, Phe, Ser, and Gly residues. The levels of ^{13}C enrichment for these residues in the purified protein varied between 65 and 90%. Details regarding the sample preparation have been given previously.[19] The sample used for recording the spectra of Figure 2 contained 4 mg of TGF-β1 in D_2O (0.8 mM dimer), p^2H 4.2, in a 200 μL Shigemi microcell (Shigemi Inc., Allison Park, Pa).

The sample of uniformly $^{13}C/^{15}N$-enriched *Xenopus* calmodulin was obtained from overexpression in *Escherichia coli*, grown on a medium containing $^{13}C_6$-glucose and $^{15}NH_4Cl$. The NMR sample contained 11 mg of protein in 390 μL of D_2O (1.7 mM), 150 mM KCl, and 1.5 mM EDTA, p^2H 6.3.

NMR spectra were recorded on a Bruker AMX-600 spectrometer, equipped with a triple-resonance probehead that contained a self-shielded z-gradient coil. TGF-β1 spectra were recorded at 45 °C and calmodulin spectra at 23 °C.

The 2D TGF-β1 spectra shown in Figure 2 each result from a 54* × 384* data matrix, with acquisition times of 12 ms (t_2) and 53 ms (t_3), keeping $t_1 = 0$. Measuring time: 4 h per spectrum. The data were apodized in the $H^{\alpha/\beta}$ dimension with a 65°-shifted sine bell window and zero-filled to 256*. In the detected dimension, data were apodized by a 65°-shifted squared sine bell window and zero filled to 1024*. The spectrum of Figure 2A was recorded with the scheme of Figure 1, keeping t_1 constant. The spectrum of Figure 2B was recorded with a single-quantum analog of the HACAHB-COSY scheme, where the ^{13}C pulses of Figure 1 were not applied (except for ^{13}C decoupling during data acquisition), and the two 90° ^{1}H pulses flanking the t_2 evolution period were incremented by 90° relative to the scheme of Figure 1. In addition, a $90°_x-90°_{\phi_3}$ pair of ^{13}C pulses ($\phi_3 = x,-x$), inserted $1/(2^1J_{CH})$ after the first ^{1}H 90_{ϕ_1} pulse, serves as a ^{13}C filter[23] (receiver = x, $2(-x),x$).

The 3D HACAHB-COSY spectrum of calmodulin results from a 50* × 54* × 384* data matrix with acquisition times of 23.2 ms (t_1), 12 ms (t_2), and 53 ms (t_3). The total number of scans for each hypercomplex t_1/t_2 increment was 32, and the total measuring time was 24 h. The data processing in the t_2 and t_3 dimensions was the same as described above for TGF-β1. In the t_1 dimension, the number of t_1 data points was doubled by mirror image linear prediction,[24] prior to cosine-squared bell apodization. The digital resolution of the final 3D spectrum was 8.4 Hz (F_1), 17.7 Hz (F_2), and 7.2 Hz (F_3).

Acknowledgment. We thank Monica L.-S. Tsang, Roger Lucas (R&D Systems, Minneapolis, MN), and Michael B. Sporn for making available the sample of TGF-β1, Hao Ren for preparing the calmodulin sample, and Dennis Torchia, Geerten Vuister, and Andy Wang for many stimulating discussions. This work was supported by the AIDS Targeted Anti-Viral Program of the Office of the Director of the National Institutes of Health.

Supplementary Material Available: The listing of the Bruker AMX pulse program for the HACAHB-COSY experiment and a figure showing strips taken from the 3D HACAHB-COSY spectrum of TGF-β1 for the residues with cross peaks in the region shown in Figure 2 of the manuscript (4 pages). This material is contained in many libraries on microfiche, immediately follows this article in the microfilm version of the journal, can be ordered from the ACS, and can be downloaded from the Internet; see any current masthead page for ordering information and Internet access instructions.

JA950096A

(20) Eggenberger, U.; Karimi-Nejad, Y.; Thüring, H.; Rüterjans, H.; Griesinger, C. *J. Biomol. NMR* **1992**, *2*, 583–590.
(21) Gemmecker, G.; Fesik, S. W. *J. Magn. Reson.* **1991**, *95*, 208–213.
(22) Emerson, S. D.; Montelione, G. T. *J. Am. Chem. Soc.* **1992**, *114*, 354–356.
(23) Otting, G.; Wüthrich, K. *Q. Rev. Biophys.* **1990**, *23*, 39–96.
(24) Zhu, G.; Bax, A. *J. Magn. Reson.* **1990**, *90*, 405–410.
(25) McCoy, M.; Mueller, L. *J. Am. Chem. Soc.* **1992**, *114*, 2108–2112.